Active point modification for sidelobe suppression with PAPR constraint in OFDM systems

Yang Zhou · Tao Jiang

Abstract In this paper, we propose an active point modification (APM) scheme to suppress the sidelobe of orthogonal frequency division multiplexing (OFDM) signals, and the key idea of APM is slightly enlarging the amplitudes of constellation points on some sub-carriers while keeping unchanged the minimum distance between constellation points. Moreover, the peak-to-average power ratio of the OFDM signal is considered. We formulate the sidelobe suppression problem by APM as a quadratically constrained quadratic programming problem, which could be solved by numerical tools. Simulation results show that APM could provide well sidelobe suppression performance while the peak-to-average power ratio could be efficiently controlled at a desired level.

Keywords OFDM · Sidelobe suppression · Active point modification (APM) · Peak-to-average power ratio (PAPR)

1 Introduction

Over the past decades, orthogonal frequency division multiplexing (OFDM) has attracted significant research interests. Since OFDM is inherently robust against the frequency-selective fading and able to transmit over non-contiguous frequency bands, it has been adopted as the physical layer technique in many communication networks [1–4]. However, due to the power leakage, the sidelobe of OFDM signals cause interferences to adjacent bands.

Y. Zhou · T. Jiang (✉)
Department of Electronics and Information Engineering,
Huazhong University of Science and Technology,
Wuhan 430074, People's Republic of China
e-mail: Tao.Jiang@ieee.org

Therefore, the sidelobe of OFDM signals should be effectively suppressed.

To suppress the sidelobe, many schemes have been proposed in the literature [5–14], which include active interference cancelation (AIC) [5–7], cancelation carrier (CC) [8], adaptive symbol transition (AST) [9], constellation adjustment (CA) [10], subcarrier weighting (SW) [11, 12], additive signal method (ASM) [13], constellation expansion (CE) [14], and spectral precoding (SP) [15]. For AIC [5–7] and CC [8], they actively transmit cancelation signals on some reserved sub-carriers, thus the data rate is reduced due to the reserved sub-carriers. For AST [9], it adds AST blocks between OFDM symbols leading to a considerable reduction of system throughput. For CA [10] and SW [11, 12], some sub-carriers are multiplied by the weights (1 or −1). Therefore, it should utilize some sub-carriers to send the side information about the selected weight to the receiver for data recovery, which results in the sub-carrier sacrifice. For ASM [13], it adds a complex-valued sequence to the original OFDM signal and thus degrades the system error performance remarkably. For CE [14], quadrature phase shift keying (QPSK) is replaced by 8-PSK, such that each point in QPSK is associated with two points in 8-PSK, then it appropriately selects one of the two points to suppress the sidelobe. The error performance thus degrades. Spectrally precoded OFDM can provide very small power spectral sidelobes [15]. However, spectral precoder incurs additional complexity in both transmitter and receiver. All these works, however, either reduce the data rate or degrade the system error performance.

In this paper, we propose a novel method, named as active point modification (APM), to suppress the sidelobe of OFDM signals. The advantages of the proposed APM method are given as: (1) Compared to AIC [5–7], CC [8], AST [9], CA [10], and SW [11, 12], it does not reduce the

data rate; (2) compared to ASM [13] and CE [14], it does not degrade the system error performance. The key idea of APM is slightly enlarging the amplitudes of constellation points on some sub-carriers to suppress the sidelobe while keeping unchanged the minimum distance between constellation points to guarantee the bit error rate (BER) performance. For convenience, we call the amplitude enlarged constellation points as active points. As a matter of course, the following natural questions arise: How to search the active points for each OFDM signal; how to decide the amplitude enlarging size for each active point. These questions will be addressed in this paper. We formulate the sidelobe suppression problem with APM as a quadratically constrained quadratic programming (QCQP) problem. Moreover, since peak-to-average ratio (PAPR) is a key challenge for OFDM signals, we consider the PAPR issue

$$
\begin{aligned}
x_n &= \frac{1}{\sqrt{N}} \sum_{k \in \mathcal{R}_s} X_k \exp\left(j2\pi k \frac{n \triangle f}{f_s} \right) \\
&= \frac{1}{\sqrt{N}} \sum_{k \in \mathcal{R}_s} X_k \exp\left(j2\pi k \frac{n}{N} \right), \quad 0 \le n \le N-1.
\end{aligned}
\tag{1}
$$

where X_k denotes the modulation data on the kth sub-carrier, $\mathcal{R}_s = \{0, \ldots, a-2, b, \ldots, N-1\}$ is the subset that consists of indexes of the data sub-carriers, $\triangle f$ is the frequency interval between adjacent sub-carriers, and $f_s = N \triangle f$ is the total bandwidth. Let $X = [X_0, \ldots, X_{a-2}, X_b, \ldots, X_{N-1}]^\top$ denote the input OFDM data block, the matrix representation of x then could be expressed as

$$
x = E_f X,
\tag{2}
$$

where E_f is an $N \times (N-L)$ matrix, shown as

$$
E_f = \frac{1}{\sqrt{N}}
\begin{pmatrix}
e^{j0\frac{2\pi}{N}0} & \cdots & e^{j0\frac{2\pi}{N}(a-2)} & e^{j0\frac{2\pi}{N}b} & \cdots & e^{j0\frac{2\pi}{N}(N-1)} \\
e^{j1\frac{2\pi}{N}0} & \cdots & e^{j1\frac{2\pi}{N}(a-2)} & e^{j1\frac{2\pi}{N}b} & \cdots & e^{j1\frac{2\pi}{N}(N-1)} \\
\vdots & \ddots & \vdots & \vdots & \ddots & \vdots \\
e^{j(N-1)\frac{2\pi}{N}0} & \cdots & e^{j(N-1)\frac{2\pi}{N}(a-2)} & e^{j(N-1)\frac{2\pi}{N}b} & \cdots & e^{j(N-1)\frac{2\pi}{N}(N-1)}
\end{pmatrix}.
\tag{3}
$$

in QCQP problem. Simulation results show that APM provides well sidelobe suppression performance and keeps the PAPR of the sidelobe-suppressed OFDM signal lower than or equal to that of original OFDM signal.

The rest of the paper is organized as follows. In Sect. 2, the system model is given. The proposed APM scheme is presented in Sect. 3. In Sect. 4, the PAPR issue is considered. The conclusions are drawn in Sect. 5.

Notations: The conjugate, transpose, and Hermitian transpose are denoted by $(\cdot)^*$, $(\cdot)^\top$, and $(\cdot)^H$, respectively. Let $\mathrm{Re}(\cdot)$ and $\mathrm{Im}(\cdot)$ be the real part and imaginary part, respectively. A diagonal matrix with the elements of vector x as diagonal entries is denoted as $\mathrm{Diag}(x)$.

2 System model

We first briefly describe the OFDM system. As shown in Fig. 1, suppose that there exists N sub-carriers, $L = (b - a + 1)$ sub-carriers in the target band have been occupied by other users and thus are turned off, the remaining $N - L$ sub-carriers are used for data transmission. The OFDM signal $x = [x_0, x_1, \ldots, x_{N-1}]$ in the time domain could be cast as

Next, we give the measurement of the sidelobe power, which is similar as those in [5–7]. The sidelobe power in the target band is measured by the sidelobe at the sample points $\{f_1, f_2, \ldots, f_P\}$, which is given by

$$
Y_p = \frac{1}{\sqrt{N}} \sum_{n=0}^{N-1} x_n \exp\left(-j2\pi n \frac{f_p}{f_s} \right), \quad p = 1, 2, \ldots, P.
\tag{4}
$$

In this paper, the sampling points are from $(a-1)\triangle f$ to $(b-1)\triangle f$ with the equivalent space of $\frac{\triangle f}{4}$. Thus we have $P = 4L$. Similarly, the matrix representation of $Y = [Y_1, Y_2, \ldots, Y_P]$ could be obtained as
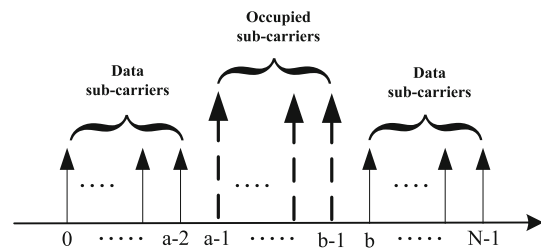
$$
Y = E_t x,
\tag{5}
$$

Fig. 1 The OFDM systems

where E_t is a $P \times N$ matrix, and the element of E_t at the pth row and nth column could be given as $\frac{1}{\sqrt{N}} \exp(-j2\pi n \frac{f_p}{f_s})$

Combining (2) and (5), the relationship between X and Y is

$$Y = EX, \tag{6}$$

where $E = E_t E_f$. Therefore, the total sidelobe power in the target band is measured by $\|Y\|_2^2$.

3 The proposed APM scheme

In this section, the proposed APM scheme is presented. The key idea of APM is easily explained in the case of quadrature phase-shift keying (QPSK) constellation, as shown in Fig. 2. For each sub-carrier, there are four constellation points (black points) in the constellation, the minimum distance between constellation points is d. If the amplitude of a point (black point) is slightly enlarged to get the modified point (white point), the minimum distance among the white point and the other three black points is also equal to d, which can guarantee the BER performance at the receiver. Therefore, for some sub-carriers, if the amplitudes of their constellation points are intelligently enlarged, the sidelobe in the target band could be suppressed and the BER performance could be guaranteed since there is no reduction of the minimum distance. In this section, we first illustrate APM for the constant modulus constellation case, then we extend it to the non-constant modulus constellation case.

3.1 APM for constant modulus constellation

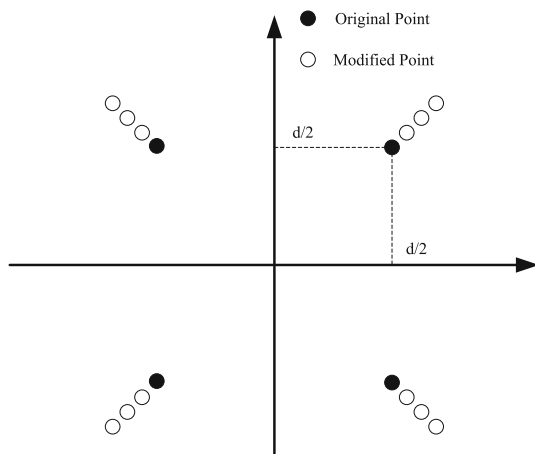In this subsection, the QPSK constellation is employed to show the principle of the proposed APM scheme.

Fig. 2 The constellation with the proposed APM method

According to Fig. 2, enlarging the amplitude of X_k is equivalent to multiply X_k by a real size C_k, satisfying $C_k \geq 1$. Therefore, the new generated data block $\bar{X} = [\bar{X}_0, \ldots, \bar{X}_{a-2}, \bar{X}_b, \ldots, \bar{X}_{N-1}]^\top$ with APM could be obtained as

$$\bar{X}_k = C_k X_k. \tag{7}$$

Define $C = [C_0, \ldots, C_{a-2}, C_b \ldots, C_{N-1}]^\top$ and $S = \text{Diag}(X)$. The new generated data block $\bar{X}$ could be rewritten as

$$\bar{X} = SC. \tag{8}$$

Combining (6) and (8), the sidelobe power with APM in the target band is measured by $\|E\bar{X}\|_2^2 = \|ESC\|_2^2$.

Based on above discussion, the sidelobe suppression problem could be cast as

$$\min_C \quad \|ESC\|_2^2$$
$$\text{s. t.} \quad C_k \geq 1, k \in \mathcal{R}_s. \tag{9}$$

In (9), $\|ESC\|_2^2 = C^\top \Psi C$ with $\Psi = S^H E^H ES$. It is worth noting that $C^\top \Psi C$ is a real number. As such, we have $C^\top \text{Im}(\Psi) C = 0$. By employing $\Phi = \text{Re}(\Psi)$, we obtain $\|E_I SC\|_2^2 = C^\top \Psi C = C^\top \text{Re}(\Psi) C = C^\top \Phi C$.

Proposition 1 Φ *is a real symmetric positive semi-definite matrix.*

Proof Define $U = \text{Re}(S^H E^H)$, and $V = \text{Im}(S^H E^H)$. Then, Ψ could be rewritten as $\Psi = (U + jV)(U^\top - jV^\top)$. Since $\Phi = \text{Re}(\Psi)$, we have $\Phi = UU^\top + VV^\top$. For any nonzero $(N - L) \times 1$ real vector y, we could obtain

$$\begin{aligned} y^\top \Phi y &= y^\top UU^\top y + y^\top VV^\top y \\ &= (U^\top y)^\top U^\top y + (V^\top y)^\top V^\top y \\ &\geq 0. \end{aligned} \tag{10}$$

Thus, it is concluded that Φ is a real symmetric positive semi-definite matrix. $\square$

As a result, (9) is equivalent to

$$(\text{P1}): \quad \min_C \quad C^\top \Phi C \tag{11a}$$
$$\text{s. t.} \quad C_k \geq 1, k \in \mathcal{R}_s. \tag{11b}$$

In above Problem, the objective function is convex since Φ is a real symmetric positive semi-definite matrix. Meanwhile, the inequality constraints are linear. Clearly, Problem (P1) is a quadratic programming (QP) problem since it minimizes a quadratic objective function over a group of linear constraints on C [18].

It is observed from Problem (P1) that APM will increase the average power since it enlarges amplitudes of the active points. To control the increasing of the average power at a desired level, we consider the average power

constraint in Problem (P1). Denote $\bar{\boldsymbol{x}} = \boldsymbol{E}_f \boldsymbol{SC}$ as the sidelobe-suppressed OFDM signal by APM. Let $\mathbf{P}_{avg}$ be the average power of $\boldsymbol{x}$, and $\bar{\mathbf{P}}_{avg}$ be the average power of $\bar{\boldsymbol{x}}$, which is cast as

$$\bar{\mathbf{P}}_{avg} = \frac{(\boldsymbol{SC})^H (\boldsymbol{SC})}{N} = \frac{(\boldsymbol{C}^H \boldsymbol{S}^H \boldsymbol{SC})}{N} = \frac{(\boldsymbol{C}^\top \boldsymbol{\Sigma} \boldsymbol{C})}{N}, \quad (12)$$

where $\boldsymbol{\Sigma} = \boldsymbol{SS}^H$ is a diagonal positive semi-definite matrix. Suppose that the increased average power is controlled at a predefined level of γ_0, i.e.,

$$\frac{\bar{\mathbf{P}}_{avg} - \mathbf{P}_{avg}}{\mathbf{P}_{avg}} \leq \gamma_0, \quad (13)$$

which is equivalent to $\bar{\mathbf{P}}_{avg} \leq (1 + \gamma_0) \mathbf{P}_{avg}$.

Therefore, when considering the increased average power constraint, the optimization problem could be formulated as

$$(P2): \quad \min_{\boldsymbol{C}} \quad \boldsymbol{C}^\top \boldsymbol{\Phi} \boldsymbol{C} \quad (14a)$$
$$\text{s. t.} \quad C_k \geq 1, \quad k \in \mathcal{R}_s, \quad (14b)$$
$$\boldsymbol{C}^\top \boldsymbol{\Sigma} \boldsymbol{C} \leq N(1 + \gamma_0) \mathbf{P}_{avg}. \quad (14c)$$

Obviously, Problem (P2) could be considered as a QCQP problem since it minimizes a quadratic objective function over a quadratic constraint and a group of linear constraints on $\boldsymbol{C}$ [18]. Problem (P2) could be effectively solved by optimization tools, e.g., CVX, a Matlab-based optimization software [19].

Remark 1 In Problem (P2), the optimal $\boldsymbol{C}^*$ must satisfy $\frac{\boldsymbol{C}^{*\top} \boldsymbol{\Sigma} \boldsymbol{C}^*}{N} = (1 + \gamma_0) \mathbf{P}_{avg}$, i.e., $\bar{\mathbf{P}}_{avg} = (1 + \gamma_0) \mathbf{P}_{avg}$; otherwise, we could scale up $\boldsymbol{C}$ such that the objective function is decreased.

In Fig. 3, the normalized power spectrums (NPSs) for different schemes are given, where $N = 128$, the target band is from $59 \triangle f$ to $88 \triangle f$, and QPSK is adopted. We present the curves of turning off, CE, CA, and CC with the goal of comparison. For APM, the average power constraint is set as $\gamma_0 = 0.5$; for CE [14], we appropriately select one of the two points in 8-PSK to suppress the sidelobe; for CA [10], we multiply each sub-carrier by sub-carrier weights (1 or -1) for the sidelobe suppression; for CC [8], the number of reserved sub-carriers is equal to 10. It can be seen that CE, CA, CC and APM can provide 5, 7, 13 and 15 dB sidelobe suppression gain, respectively, compared to turning off. Actually, CE and CA are both phase rotation schemes. For some sub-carriers, rotating their points' phases does not change the amplitudes of their sidelobes, leading to the poor performance. CC inserts some signals on the reserved sub-carriers which are on the edge of the target band, the sidelobes of these reserved sub-carriers can be utilized for canceling the power leakage in

the target band. For APM, enlarging the amplitudes of some points is equivalent to enlarging their sidelobes, these amplitude enlarged sidelobes can thus be utilized to cancel the power leakage. Therefore, CC and APM can both provide well sidelobe suppression performances. In addition, we see that the spectrums of APM on the edge of the target band have been enlarged. This is because the amplitudes of the points on these sub-carriers have been enlarged. While, for CE and CA, since they only rotate the phase of some points, the spectrums on the edge of the target band thus remain unchanged. Actually, APM with adjustable γ_0 provides distinct suppression performances, which is shown in Fig. 4. It can be observed that APM could obtain spectrum notches depth about 5, 15, and 18 dB for $\gamma_0 = 0.1, 0.5$, and 1.0, respectively. The reason is that more power means more flexibility, which then results in a better suppression performance.

3.2 APM considering complexity issue

In Problem (P2), there exists $(N - L)$ variables in (14b). The computation complexity increases as $(N - L)$ increases. Actually, the number of variables can be reduced to lower the complexity. Meanwhile, the sidelobe suppression performance could be achieved with an acceptable loss, which is described in the following argument. Let $\mathcal{R}_{s'} = \{a - 1 - \frac{M}{2}, \ldots, a - 2, b, \ldots, b - 1 + \frac{M}{2}\}$ be the index set of the sub-carriers which are close to the target band with M being a given integer, while let $\mathcal{R}_{s'}^c = \{0, \ldots, a - 2 - \frac{M}{2}, b + \frac{M}{2}, \ldots, N - 1\}$ be the index set of the sub-carriers that are away from the target band. Given the fact that the sub-carriers in $\mathcal{R}_{s'}$ introduce more sidelobe power than those in $\mathcal{R}_{s'}^c$, so if we search the active points only in $\mathcal{R}_{s'}$, i.e., $C_k \geq 1, k \in \mathcal{R}_{s'}$ and $C_k = 1, k \in \mathcal{R}_{s'}^c$, the suppression performance loss is acceptable while the complexity can be significantly reduced.

When considering the complexity issue, the QCQP formulation can be expressed as

$$(P3): \quad \min_{\boldsymbol{C}} \quad \boldsymbol{C}^\top \boldsymbol{\Phi} \boldsymbol{C} \quad (15a)$$
$$\text{s. t.} \quad C_k \geq 1, \quad k \in \mathcal{R}_{s'}, \quad (15b)$$
$$C_k = 1, \quad k \in \mathcal{R}_{s'}^c, \quad (15c)$$
$$\boldsymbol{C}^\top \boldsymbol{\Sigma} \boldsymbol{C} \leq N(1 + \gamma_0) \mathbf{P}_{avg}. \quad (15d)$$

Comparing (14b) with (15b), it can be seen that the number of variables has been reduced from $(N - L)$ to M, resulting in the reduction of the complexity. Note that, when $\mathcal{R}_{s'}$ and $\mathcal{R}_{s'}^c$ are given, they will be used for all the input X.

The NPSs with APM when considering the complexity issue are presented in Fig. 5, where $N = 128$, the target band is from $59 \triangle f$ to $88 \triangle f$, $\gamma_0 = 0.5$ for APM, and QPSK is selected. The curve labeled with "NO" means the

Fig. 3 NPSs for different schemes, QPSK
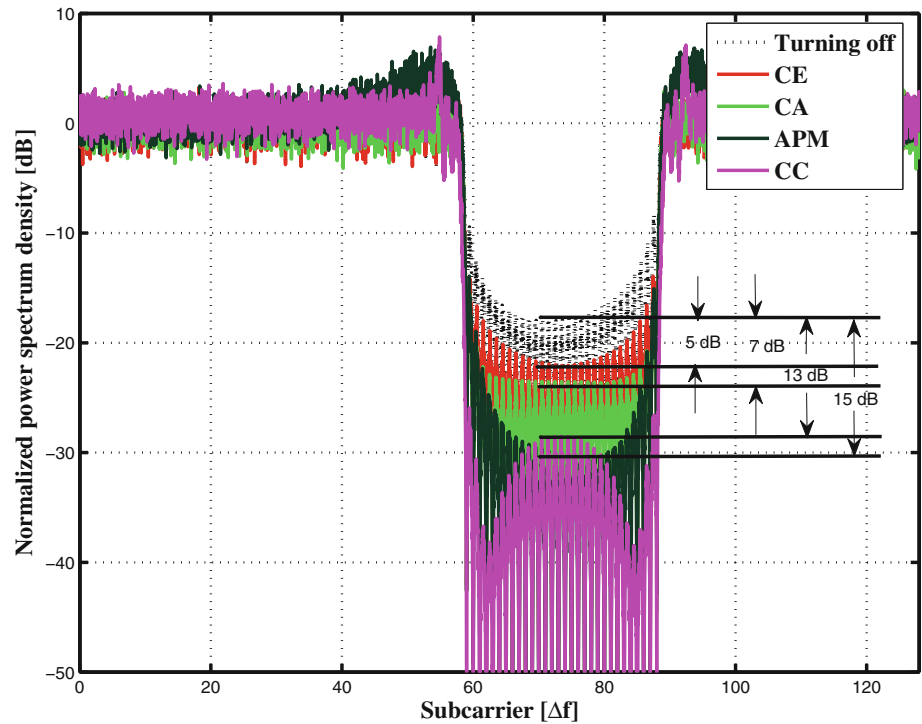
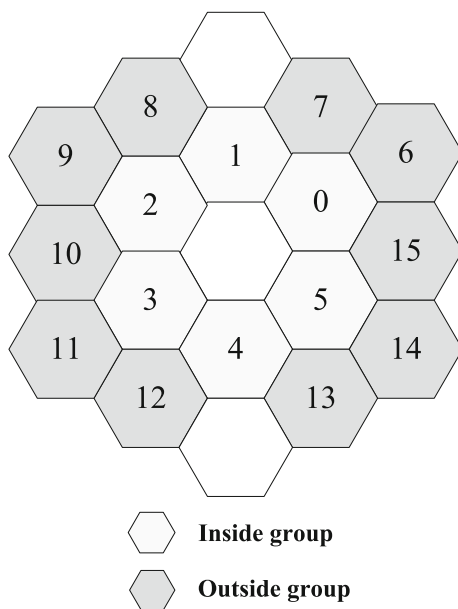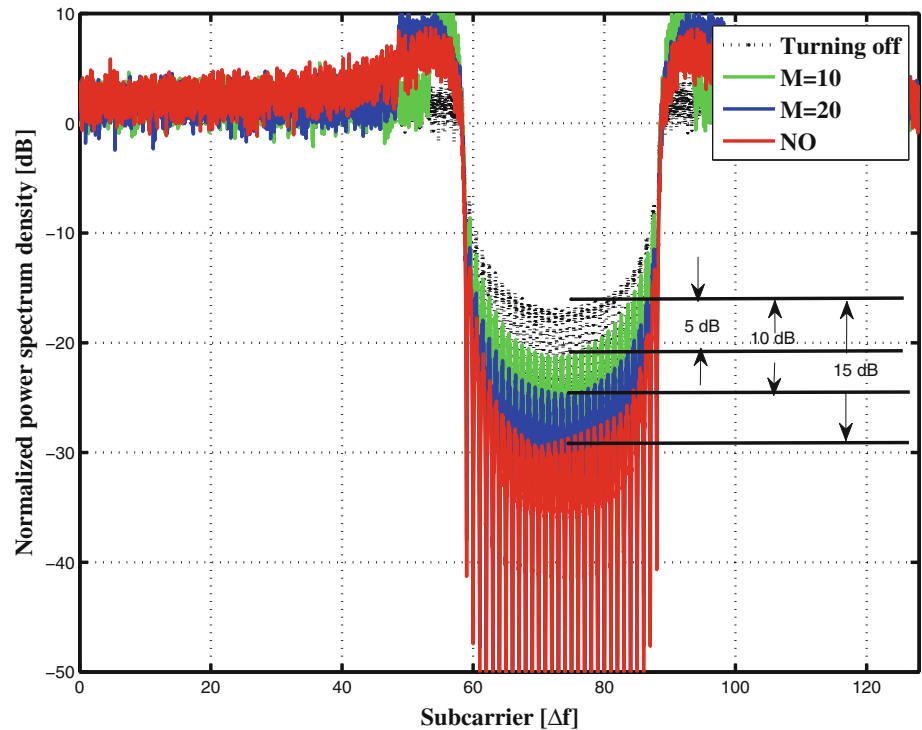
Fig. 4 NPSs for APM with different γ_0, QPSK
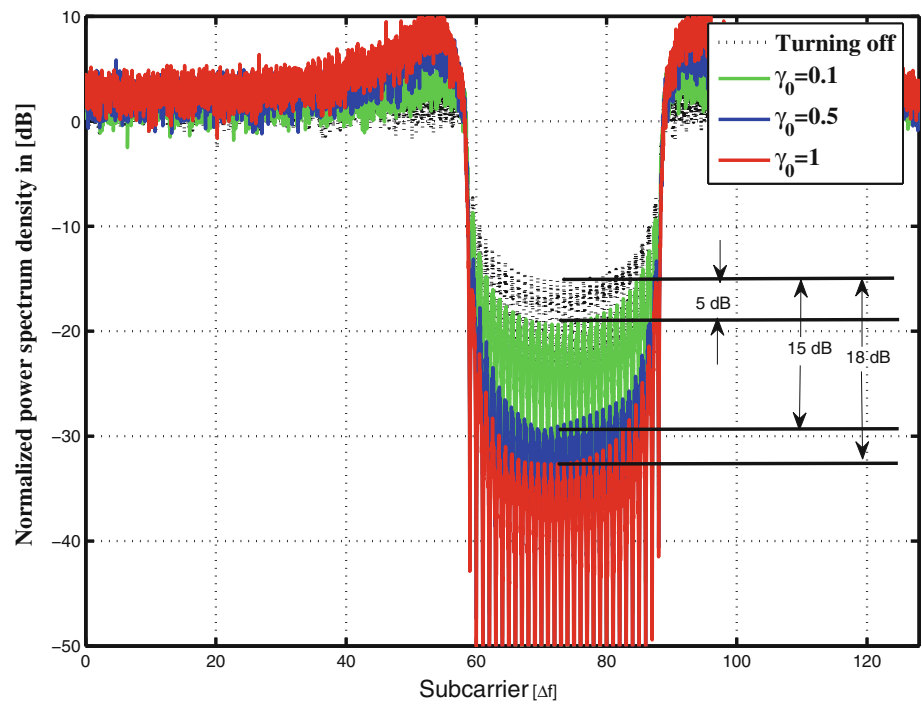
complexity issue is not considered. It can be seen that the sidelobe suppression performance increases as M increases. When $M = 20$, the complexity has been largely reduced because the number of inequality constraints have been reduced from 98 to 20, and the suppression performance losses only 5 dB compared to the curve labeled with "NO".

3.3 APM for non-constant modulus constellation

In this subsection, we consider the non-constant modulus constellation. Since hexagonal constellation is denser than square constellation in the plane, some researchers have adopted the hexagonal (HEX) constellation in OFDM systems [16]. As such, the 16 hexagonal constellation (16

Fig. 5 NPSs for APM with $\gamma_0 = 0.5$ and different M, QPSK

points' amplitudes like the case of constant modulus constellation. For convenience, denote $\mathcal{R}_{so}, \mathcal{R}_{si}$ as the index sets of the outside group points and inside group points in X, respectively. It is worth noting that $\mathcal{R}_{so}$ and $\mathcal{R}_{si}$ could be obtained when X is generated. For different X, the two sets may be different.

The sidelobe suppression problem with APM for the non-constant modulus constellation case could be formulated as

$$(P4): \quad \min_{C} \quad C^\top \Phi C \tag{16a}$$

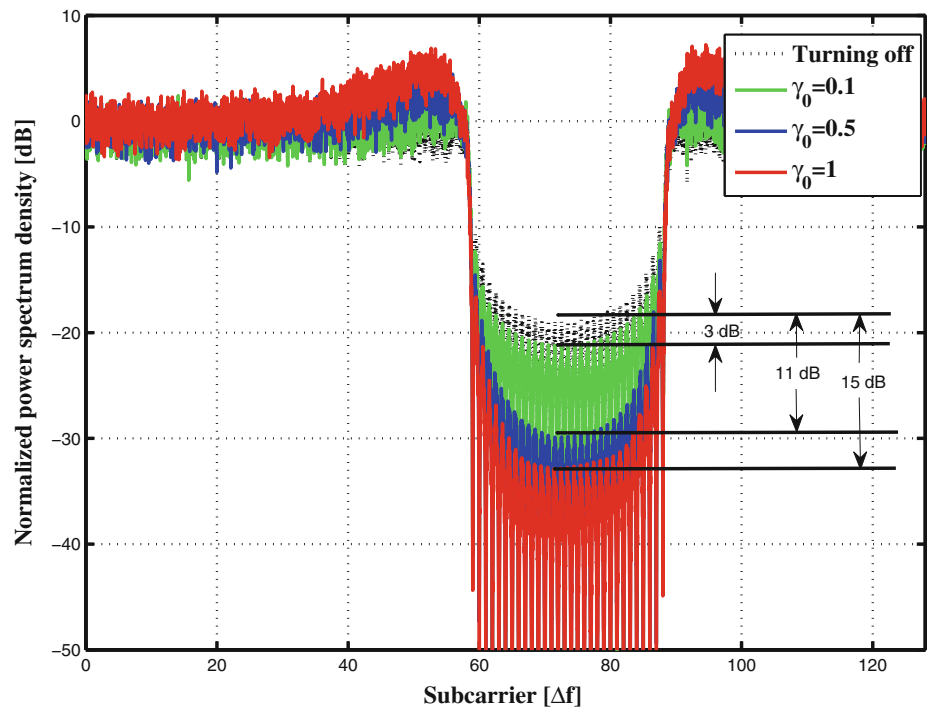$$\text{s. t.} \quad C_k \geq 1, \quad k \in \mathcal{R}_{so}, \tag{16b}$$

$$C_k = 1, \quad k \in \mathcal{R}_{si}. \tag{16c}$$

In Problem (P4), (16b) means that the active points only locate in the outside group, and (16c) ensures that the inside group points remain unchanged. Similar to Problem (P3), the average power constraint and the complexity issue also could be introduced. Due to space limitation, they are omitted in this paper.

In Fig. 7, we plot the NPSs using APM for different γ_0, where $N = 128$, the target band is from $59\triangle f$ to $88\triangle f$, and 16 HEX is selected. Note that the complexity issue is not considered. Similarly, APM with distinct γ_0 could provide different performances. The bigger γ_0 is, the better performance is. Comparing Figs. 4 and 7, it is observed that the performance of 16 HEX is slightly worse than that of QPSK. The reason is that the inside group points in non-constant modulus constellation cannot be enlarged.

Fig. 6 The 16 HEX constellation

HEX) is adopted as an example in this subsection, as shown in Fig. 6. The 16 points are first divided into two groups: one is named as inside group including 6 inner points, the other is named as outside group including 10 outer points. We keep unchanged the inside group points since the minimum distance will be reduced if we enlarge their amplitudes. Meanwhile, we enlarge the outside group

**Fig. 7** NPSs for APM with different γ_0, 16 HEX

However, we could enlarge all the points in constant modulus constellation.

3.4 Combining APM And CA for higher order constellation

In this subsection, the combination of APM and CA [10] is considered for higher order (≥ 64) constellation. Due to the multiplication of some sub-carriers by weights {1 or −1}, the side information in CA about the adjustment should be sent to the receiver for data recovery. Thus, there is sub-carriers sacrifice. However, if APM and CA are combined for high order hexagonal constellations, the side information is not needed and the sidelobe can be deeper suppressed than that using APM, which is shown as follows.

With the same minimum distance d between points, we can pack more points with hexagonal constellation in a given area than that with quadratic amplitude modulation (QAM) constellation. The extra degrees of freedom by using hexagonal constellation instead of QAM constellation can be utilized to eliminate the side information. 64 HEX is employed as an example to illustrate this principle, as shown in Fig. 8, where the 91 points are divided into three groups, named as inner group, midterm group, and outside group, respectively. For inner group points ('0','1',...,'6') and outside group points ('34','35',...,'63'), they have 1 representation; for midterm group points ('7','8',...,'33'), they have two 2 representations, e.g., both the points 7a and 7b represent the same one of '7'. As such,
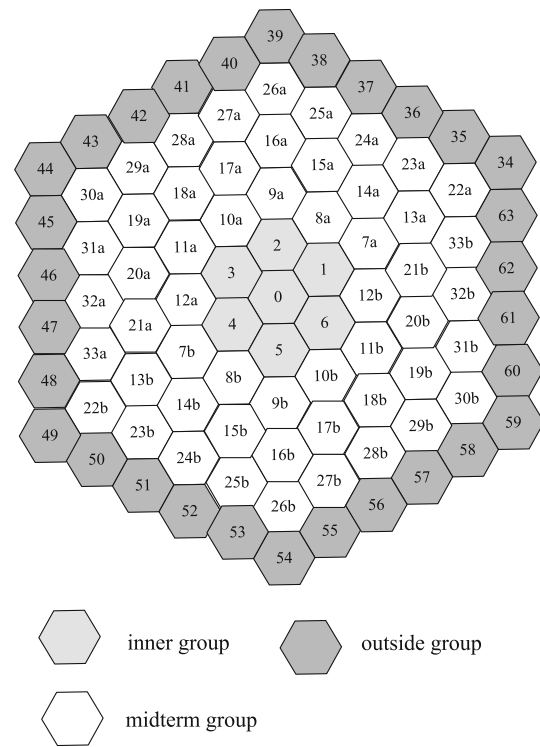
Fig. 8 The 64 HEX constellation

we appropriately choose one representation for midterm group points to suppress the sidelobe. At the receiver, either 'la' and 'lb' can be considered as 'l', for $l = 7, 8, \ldots, 33$. Based on above discussion, the side information can be eliminated. When combining APM and CA (APM-CA), CA
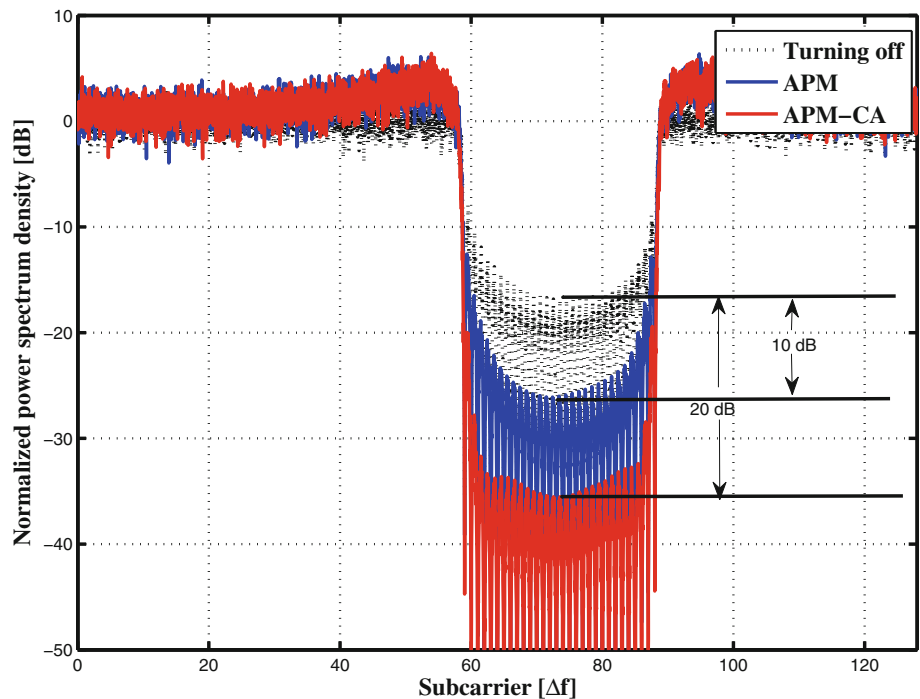
is firstly employed to adjust the midterm group points to
suppress the sidelobe and keep unchanged the inner group
points, APM is then employed to enlarge the amplitudes of
outside group points to improve the performance.

Figure 9 shows the NPSs for APM and APM-CA, where
$N = 128$, the target band is from $59\triangle f$ to $88\triangle f$, $\gamma_0 = 0.5$
for APM, and 64 HEX is selected. Note that the complexity
issue is not considered. It is observed that APM provides
10 dB sidelobe suppression gain compared to turning off,
while APM-CA can improve the performance about 10 dB
compared to APM.

Remark 2 Since APM does not reduce the minimum
distance, the BER performance can be guaranteed at the
receiver. Given the fact from Remark 1 that $\bar{\mathbf{P}}_{avg} =
(1 + \gamma_0)\mathbf{P}_{avg}$, the cost of APM is the increased average
power. One step further, if we want to keep the average
power unchanged with APM processing, we should scale $\bar{x}$
with a factor $\sqrt{\frac{1}{1+\gamma_0}}$, which will result in the BER perfor-
mance degradation because the minimum distance is
reduced from d to $\frac{d}{\sqrt{1+\gamma_0}}$.

We first plot the comparison of BER performances for
different schemes when Gaussian channel is adopted in
Fig. 10. The parameters are the same as Fig. 3. We see that
CA and CC do not affect the BER performance, but they
both reduce the data rate due to the sub-carriers sacrifice. In
addition, the curve of CE degrades about 3.8 dB when
BER $= 10^{-4}$, this is a consequence of the replacement of
QPSK by 8-PSK. For APM, its BER performance is almost

the same as that of turning off since it keeps the minimum
distance unchanged. We then show the BER performance
of APM with normalization for different constellations in
Fig. 11, where the Gaussian channel is adopted, $N = 128$,
the target band is from $59\triangle f$ to $88\triangle f$, and $\gamma_0 = 0.25$. Note
that the complexity issue is not considered. For each con-
stellation, there are three curves, turning off, APM and
APM with normalization, respectively. Here, APM with
normalization means that $\bar{x}$ is scaled by $\sqrt{\frac{1}{1+\gamma_0}}$. It can be
seen that the BER performance of APM with normalization
degrades about 0.7 dB when BER $= 10^{-4}$ compared to
turning off. This is because the scaling operation reduces
the minimum distance from d to $\frac{d}{\sqrt{1+\gamma_0}}$.
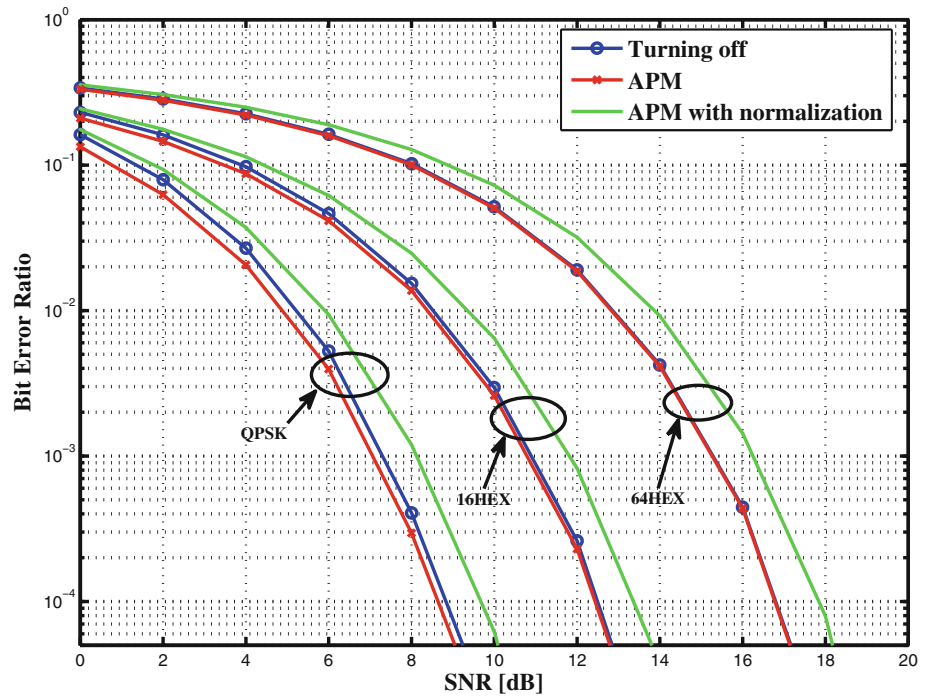
4 The PAPR issue

In this section, the PAPR issue is considered. It is well
known that one of major challenges in the design of a real
OFDM system is its high PAPR. OFDM signals with high
PAPR require the high power amplifier (HPA) with a wide
linear range. If the linear range is insufficient, the large
PAPR results in the increase of the sidelobe in the target
band. Even if the sidelobe has been suppressed by APM, it
still increases after being amplified by the HPA with a
insufficient linear range. Therefore, the PAPR issue should
be considered for the sidelobe suppression problem. The
formulation of the constant modulus constellation case is
very similar to the non-constant modulus constellation

Fig. 10 BER versus SNR for different schemes, QPSK
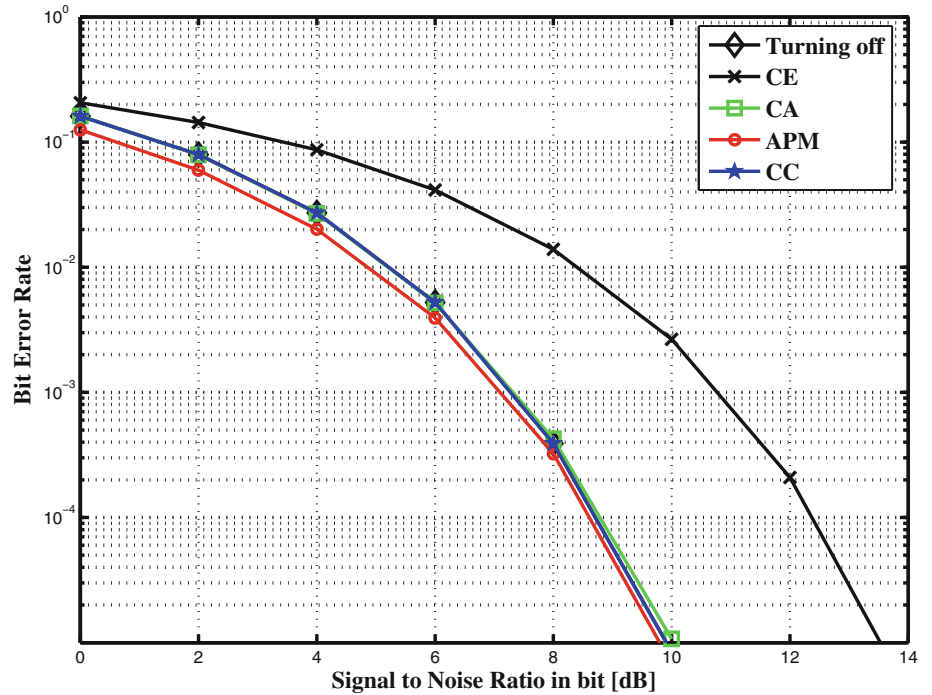
Fig. 11 BER versus SNR for APM with normalization, $\gamma_0 = 0.25$

case, so constant modulus constellation is adopted to show the principle in this section.

The PAPR of original OFDM signal $\boldsymbol{x}$ is defined as

$$\text{PAPR}\{\boldsymbol{x}\} = \frac{\|\boldsymbol{x}\|_\infty^2}{\frac{1}{N}\|\boldsymbol{x}\|_2^2}, \tag{17}$$

where $\|\boldsymbol{x}\|_\infty = \max(|x(1)|, |x(2)|, \ldots, |x(N)|)$. For the side-lobe-suppressed signal $\bar{\boldsymbol{x}}$, its PAPR is defined as

$$\text{PAPR}\{\bar{\boldsymbol{x}}\} = \frac{\|\bar{\boldsymbol{x}}\|_\infty^2}{\frac{1}{N}\|\boldsymbol{x}\|_2^2}. \tag{18}$$

Note that we adopt $\frac{1}{N}\|\boldsymbol{x}\|_2^2$ in the denominator of this PAPR definition. This PAPR definition avoids misleading PAPR reduction due to average power increasing and thus all the PAPR reduction must come from peak power reduction [17].

Fig. 12 NPSs for APM with $\gamma_0 = 0.5$ and different λ_0, QPSK
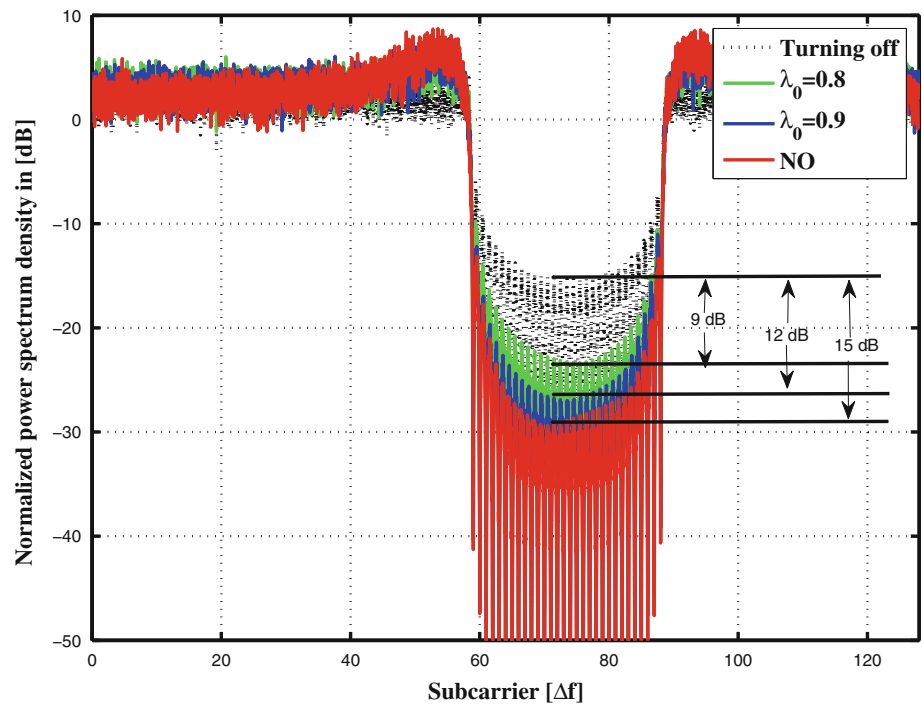
Define λ as the ratio of PAPR$\{\bar{x}\}$ to PAPR$\{x\}$, i.e.,

$$\lambda = \frac{\text{PAPR}\{\bar{x}\}}{\text{PAPR}\{x\}} = \frac{\|\bar{x}\|_\infty^2}{\|x\|_\infty^2} = \frac{\|E_f SC\|_\infty^2}{\|x\|_\infty^2}. \qquad (19)$$

We set the PAPR constraint as $\lambda \le \lambda_0$ with λ_0 being the target ratio, such that (19) is rewritten as

$$\|E_f SC\|_\infty^2 \le \lambda_0 \|x\|_\infty^2. \qquad (20)$$

It is worth noting that the PAPR of $\bar{x}$ is lower than or equal to that of x if $\lambda_0 \le 1$. Denoting e_n as the nth row of E_f, (20) is equivalent to

$$|e_n SC|^2 \le \lambda_0 \|x\|_\infty^2, n = 1, 2, \dots, N, \qquad (21)$$

with $|e_n SC|^2$ satisfying

$$|e_n SC|^2 = C^\top S^H e_n^H e_n SC = C^\top \Theta_n C, \qquad (22)$$

where $\Theta_n = \text{Re}(S^H e_n^H e_n S)$. It is worth noting that $C^\top \text{Im}(S^H e_n^H e_n S)C = 0$.

Proposition 2 $\Theta_n, n = 1, 2, \dots, N$, *are real symmetric positive semidefinite matrices.*

Proof The proof is similar to Proposition 1. □

Therefore, when considering the PAPR issue in Problem (P2), the QCQP formulation could be given by

$$(P5): \quad \min_C \quad C^\top \Phi C \qquad (23a)$$
$$\text{s. t.} \quad C_k \ge 1, k \in \mathcal{R}_s, \qquad (23b)$$
$$C^\top \Sigma C \le (1 + \gamma_0) N \mathbf{P}_{avg}, \qquad (23c)$$
$$C^\top \Theta_n C \le \lambda_0 \|x\|_\infty^2, n = 1, 2, \dots, N. \qquad (23d)$$

The NPSs of APM considering PAPR issue for distinct λ_0 are given in Fig. 12, where $N = 128$, $\gamma_0 = 0.5$, the target band is from $59\triangle f$ to $88\triangle f$, and QPSK is adopted. The curve labeled with "NO" means that the PAPR issue is not considered. It is observed that the sidelobes of APM are 9 and 12 dB lower than that of turning off when $\lambda_0 = 0.8$ and 0.9, respectively. Therefore, APM can be utilized for joint sidelobe suppression and PAPR reduction.

5 Conclusions

In this paper, a novel APM scheme was proposed to suppress the sidelobe in OFDM systems. The problem of sidelobe suppression with APM was formulated as a QCQP problem when considering the complexity and the PAPR issues, which was very meaningful in practical systems.

References

1. Mitola, J. (1999). Cognitive radio for flexible mobile multimedia communications. In *Proceedings of MoMuC*, November 1999, CA, USA.
2. Stotas, S., & Nallanathan, A. (2011). Enhancing the capacity of spectrum sharing cognitive radio networks. *IEEE Transactions on Vehicular Technology, 60*(8), 3768–3779.
3. Quan, Z., Cui, S., Sayed, A., & Poor, H. V. (2009). Optimal multiband joint detection for spectrum sensing in dynamic spectrum access networks. *IEEE Transactions on Signal Processing, 57*(3), 1128–1140.
4. Weiss, T., Hillenbrand, J., Krohn, A., & Jondral, F. (2004) Mutual interference in OFDM-based spectrum pooling systems. In *Proceedings of VTC*, May 2004, CA, USA.
5. Yamaguchi, H. (2004) Active interference cancellation technique for MB-OFDM cognitive radio. In *Proceedings of EuMW* (Vol. 2), October 2004, Amsterdam, The Netherlands.
6. Wang, Z., Qu, D., & Jiang, T. (2008). Spectral sculpting for OFDM based opportunistic spectrum access by extended active interference cancellation. In Proceedings of Globecom, November 2008, New Orleans, USA.
7. Qu, D., Wang, Z., & Jiang, T. (2010). Extended active interference cancellation for sidelobe suppression in cognitive radio OFDM systems with cyclic prefix. *IEEE Transactions on Vehicular Technology, 59*(4), 1689–1695.
8. Brandes, S., Cosovic, I., & Schnell, M. (2006). Reduction of out-of-band radiation in OFDM systems by insertion of cancellation carriers. *IEEE Communications Letters, 10*(6), 420–422.
9. Mahmoud, H. A., & Arslan, H. (2008). Sidelobe suppression in OFDM-based spectrum sharing systems using adaptive symbol transition. *IEEE Communications Letters, 12*(2), 133–135.
10. Li, D., Dai, X., & Zhang, H. (2009). Sidelobe suppression in NC-OFDM systems using constellation adjustment. *IEEE Communications Letters, 13*(5), 327–329.
11. Cosovic, I., Brandes, S., & Schnell, M. (2005). A technique for sidelobe suppression in OFDM systems. In *Proceedings of Globecom*, November 2005, St. Louis, MO.
12. Cosovic, I., Brandes, S., & Schnell, M. (2006). Subcarrier weighting: A method for sidelobe suppression in OFDM systems. *IEEE Communications Letters, 10*(6), 444–446.
13. Cosovic, I., & Mazzoni, T. (2007). Sidelobe suppression in OFDM spectrum sharing systems via additive singal method. In *Proceedings of VTC*, April 2007 (pp. 2692–2696).
14. Pagadarai, S., Rajbanshi, R., Wyglinski, A. M., & Minden, G. J. (2008). Sidelobe suppression for OFDM-based cognitive radios using constellation expansion. In *Proceedings of WCNC*, March 2008, Las Vegas, NV, USA.
15. Chung, C. D. (2008). Spectral precoding for rectangularly pulsed OFDM. *IEEE Transactions on Communications, 56*(9), 1498–1510.
16. Han, S., Cioffi, J., & Lee, J. (2008). On the use of hexagonal constellation for peak-to-average power ratio reduction of an OFDM signal. *IEEE Transactions on Wireless Communications, 7*(3), 781–786.
17. Tellado, J. (1999). Peak to average power reduction for multi-carrier modulation, Chap. 3. Ph.D. dissertation, Stanford University.
18. Boyd, S., & Vandenberghe, L. (2004). *Convex optimization*, Chap. 4, and Chap. 11. Cambridge: Cambridge University Press.
19. Grant, M., & Boyd, S. (2010). Cvx usersguide for cvx version 1.21 (build 782), May 2010. [Online]. Available: http://cvxr.com/.

Author Biographies

Yang Zhou received the B.Eng. degree in information engineering from the Wuhan University of Technology, Wuhan, P. R. China, in 2008. He is currently pursuing the Ph.D. degree at the Huazhong University of Science and Technology, Wuhan. Since September 2010, he is also with the Department of Electrical and Computer Engineering, Texas A&M University, College Station, as a visiting student. His research interests include communication theory and signal processing for wireless communications, especially for OFDM and wireless sensor networks.

Tao Jiang (M'06, SM'10) is currently a full Professor in Wuhan National Laboratory for Optoelectronics, Department of Electronics and Information Engineering, Huazhong University of Science and Technology, Wuhan, P. R. China. He received the B.S. and M.S. degrees in applied geophysics from China University of Geosciences, Wuhan, P. R. China, in 1997 and 2000, respectively, and the Ph.D. degree in information and communication engineering from Huazhong University of Science and Technology, Wuhan, P. R. China, in April 2004. From Aug. 2004 to Dec. 2007, he worked in some universities, such as Brunel University and University of Michigan in UK and USA, respectively. He has authored or co-authored over 100 technical papers in major journals and conferences and five books/chapters in the areas of communications. His current research interests include the areas of wireless communications and corresponding signal processing, especially for cognitive wireless access, vehicular technology, OFDM, UWB and MIMO, cooperative networks, smart grid and wireless sensor networks. He served or is serving as symposium technical program committee membership of many major IEEE conferences, including INFOCOM, ICC, and GLOBECOM, etc. He is invited to serve as TPC Symposium Chair for the IEEE GLOBECOM 2013 and IEEEE WCNC 2013, and as a general co-chair for the workshop of M2M Communications and Networking in conjunction with IEEE INFOCOM 2011. He is served or serving as associate editor of some technical journals in communications, including in IEEE Communications Surveys and Tutorials, IEEE Transactions on Vehicular Technology etc. He is served as guest editor of IEEE Communications Surveys and Tutorials for special issue on Energy and Smart Grid. He is a recipient of the Best Paper Awards in IEEE CHINACOM09 and WCSP09. He is a Senior Member of IEEE, Members of IEEE Communication Society, IEEE Vehicular Technology Society, IEEE Broadcasting Society, IEEE Signal Processing Society, and IEEE Circuits and Systems Society.